TECHNIUM

Technium Vol. 2, Issue 5 pp.49-61 (2020)
ISSN: 2668-778X
www.techniumscience.com

Characterization of Magnetite and Zinc Oxide Nanoparticles bio-synthesized with Snakeweed (*Stachytarpheta Indica*)

Ngwu, C. M. Nnaji, J. C. and Odoemelam, S. A.

Department of Chemistry, Michael Okpara University of Agriculture Umudike, P.M.B 7267 Umuahia, Abia State, Nigeria

E-mail: *kom4tngwu@gmail.com*

Abstract

Biosynthesis or green synthesis was employed for the preparation of magnetite and ZnO nanoparticles using non-hazardous solvents and plant extracts of snake weed. The leaf extract has shown to be rich in polyphenols, which facilitated the reduction and capping of the synthesized metal oxide nanoparticles, as indicated by the FTIR spectra. The nano-ZnO particles appeared spherical and agglomerated in structure with particle sizes of about 2-20 nm, while the bio-magnetite particles had a sheet-like layer that appeared clumped and cracked, with an SEM average grain size of 1-4 nm. The crystallite sizes were 3 and 0.026 nm for both ZnO and Iron nanocomplexes. The various elemental components of the particles in their different proportions were confirmed by the EDX spectra. The crystallinity of the nanoparticles was well defined by the very sharp and broad peaks, although capped by the biomolecules of the snake weed extract. Results indicate that the process can be used as an efficient green and economical alternative to the chemical synthesis of the same and its attendant draw-backs.

Keywords: Biosynthesis, magnetite, zinc oxide, snakeweed

1.0 Introduction

The application of nanotechnology in various fields such as environmental remediation, agriculture and biomedical sciences has been on the rise in recent times. Most metals, metal oxides and carbon based nanoparticles have been engineered to meet these specific needs. Particles having at least one dimension less than 100 nm in size are considered as nanoparticles (Thakkar *et al.,* 2010). Several synthesis methods are available for nanoparticles which include; chemical methods (Manna *et al.,* 2013; Roldán *et al*., 2013), physical methods (Abou El-Nour *et al*., 2010; Asanithi *et al.,* 2012) and biological methods (Ahmmad *et al.,* 2013, Siddiqi *et al.* 2018). These methods, excluding the biological method have major drawbacks such as the use of toxic chemicals, formation of hazardous byproducts, contaminations arising from precursor chemicals, defective surface formation, low rate of production, high cost of production, and high energy requirements (Mihir *et al.,* 2014). Hence, environmentally friendly and cost effective alternative synthesis methods are needed. Green or biosynthesis of nanoparticles is an environmentally friendly method that eliminates the use of hazardous and expensive chemicals (Nayantara, 2018). The process is simple and cost-effective with zero contamination, capping and reduction ability, high reducing potential, high scale up capacity and surface fine-tuning. Biosynthesis uses bacteria, plant extracts and fungi along with the precursors to produce nanoparticle instead of conventional chemicals for bio reduction and capping purposes.

Synthesis of metal nanoparticles exploiting plant extracts is very economical, and therefore, can be used as a cost effective and important option for the extensive production of metal nanoparticles. The widespread occurrence of biomolecules such as polyphenolic, hydroxyl,

Technium Vol. 2, Issue 5 pp.49-61 (2020)
ISSN: 2668-778X
www.techniumscience.com

alkyne, carboxyl, and amide groups of the monoterpenoids, sesquiterpenes, and phytols in plant extracts could explain their ability to reduce metal ions. Also, the biomolecules of plant extract attaches chemically to the surface of the nano-structures, to stabilize the nanoparticles and impede their aggregation (Ghorbani *et al.*, 2015). The biosynthesized nanoparticles have unique and enhanced properties that find its way in various useful applications, including nano-remediation of environmental matrices (Shah *et al.*, 2015). Currently, the number of reports on green-synthesized nanoparticles is on the increase. Extracts derived from diverse plant species, their organs, and isolated compounds are being successfully used in the green synthesis of NPs.

Stachytarpheta indica (L.) Vahl (snake weed) is a much branched, herb species of *Verbenaceae* family found in many continents, and popular in West Africa. Studies have been documented literature referring to many of its biological activities e.g. wound healing, antimicrobial activity, hepatoprotection, hypoglycemic activity, and cardiovascular effects (Sahoo *et al.*, 2014). The Leaf and stem of the plant have been reported to be rich in phytochemicals like alkaloid, saponins, tannins and phlobotanins (Félicien, 2016). These phytochemicals have characteristics which can make them function as green stabilizers, emulsifiers and reducing agents in the synthesis of nanoparticles without using hazardous chemicals. Based on existing literature, there are still no specific researches using *S. indica* for nanoparticles synthesis and this work focuses on the biosynthesis of Fe_3O_4 and ZnO nanoparticles with the leaf extract of the plant.

2.0 Materials and Methods

2.1. Materials

Fresh leaves of *S. indica* were collected from Michael Okpara University of Agriculture, Umudike (MOUAU) and identified by the Forestry Department, MOUAU. Analytical grade zinc acetate dihydrate [$Zn(CH_3COO)_2.2H_2O$] crystals, iron (II) chloride tetrahydrate ($FeCl_2.4H_2O$), iron (III) chloride hexahydrate ($FeCl_3.6H_2O$) and sodium hydroxide (NaOH) were procured from BDH Chemicals Limited, Poole, England.

2.2 Preparation of *S. indica* Extract

Leaf samples were washed thoroughly 3 times with clean water and rinsed with distilled water. The leaves were allowed to dry at room temperature (32 ^oC) and 40 g were boiled in 200 mL of double distilled water for 20 min at 60 ^oC. The light yellow coloured solution formed was allowed to cool to room temperature. The solution was filtered with 0.5 mm Whatman no. 41 filter paper and stored in the refrigerator.

2.3 Biosynthesis of ZnO nanoparticles

The biosynthesis of ZnO nanoparticle was carried out using the methods described by Sangeetha *et al.* (2011) and Gnanasangeetha and Thambavani (2013a). *S. indica* aqueous extract (140 mL) was taken from the stock solution and 14 g of zinc acetate dihydrate crystals was dissolved in it under constant stirring using magnetic stirrer. After complete dissolution of the crystals, the solution was allowed to boil at 70 °C by using magnetic stirrer until the formation of a deep yellow colored paste. The paste was then transferred to a ceramic crucible cup and heated in a laboratory furnace (HMG, India) at 400 ^oC for 2 h. The light yellow coloured powder obtained was used for characterization studies.

Technium Vol. 2, Issue 5 pp.49-61 (2020)
ISSN: 2668-778X
www.techniumscience.com

2.4 Bio-synthesis of magnetite

A slight modification of the method of Mahdavi *et al.* (2013), was employed for the synthesis of *S. indica*/Fe_3O_4-NPs. Firstly, a solution of Fe^{3+} and Fe^{2+} salts in a 2:1 M ratio was added to the snakeweed extract (20 mL) to obtain a yellowish colloidal solution. Then, a freshly prepared 1.0 M solution of NaOH was added drop-wise to the solution under continuous stirring. The pH of the solution was adjusted to 11. The solution was then stirred for 1 h for complete homogenization. The Fe_3O_4-NPs formed was severally washed with deionized water. The nanoparticles were dried in an oven at 70 °C for 24 h. The dried sample was stored in an air-tight container for further characterization.

2.4 Characterization of Nanoparticles

2.4.1 X-ray diffraction (XRD)

The crystalline forms of the nanoparticles were quantified by measuring their X-ray diffraction patterns, recorded using a high-resolution Bruker D8 Advance diffractometer of Cu Kα (λ = 1.54050 Å) radiation. The samples (1 g) were scanned from 15° to 90° 2 Theta range with a step size of 0.02° and a step rate of 0.454° s^{-1}. The crystallite size was calculated from the XRD pattern with the help of the Debye-Scherrer equation given as, $D = K\lambda / \beta\cos\theta$ where D is crystallite size (nm), λ is the wavelength of X-rays (1.54050 Å), β exhibits the full width of the peak at half maximum (FWHM) and cos θ is Bragg angle (rad). K is Scherrer constant (0.94) related to crystallite shape.

2.4.2 FTIR Analysis

Infrared spectra were obtained by using a Fourier transform infrared spectrometer (FTIR) (Perkin-Elmer Spectrum RX1). The analysis was performed to confirm the presence of surface functional groups. The powder samples (99 mg) were mixed well with 1 mg of potassium bromide (KBr) and pressed into pellets under vacuum, until they appeared clear and not translucent. The pellets were then carefully removed from the disc, placed in the FTIR sample holder and analyzed by the transmission mode with a resolution of 4 cm^{-1}. The spectra of the different samples were recorded in the wavenumber range of 4000 to 400 cm^{-1}.

2.4.3 FE-SEM/EDX Analysis

The surface morphology of synthesized nanoparticles at different magnifications was studied using Field emission scanning electron microscopy equipped with an energy dispersive X-ray (EDX) detector (FESEM) (ZEISS ultra plus). To be observed with a SEM, 20 mg of the samples were first made conductive for current. This was done by coating them with an extremely thin layer (1.5 - 3.0 nm) of gold-palladium for sputtering.

Technium Vol. 2, Issue 5 pp.49-61 (2020)
ISSN: 2668-778X
www.techniumscience.com

3.0 Results and Discussion

3.1 FESEM Analysis

3.1.1 FESEM with EDX images of bio-ZnO nanoparticles

The FESEM images of the synthesized bio-ZnO nanoparticles with different magnifications are shown in Fig. 1 (a-b), which reveals that the bio-ZnO nanoparticles were spherical and globular with higher degree of agglomeration compared to ZnO. These images also indicate the availability of nano-size pores and cracks on the surface of the nanoparticles. Detailed structural characterizations demonstrate that the synthesized products were spherical and crystalline in structure and their particle sizes were about 2-20 nm. Particle sizes obtained from SEM images are usually larger than those of XRD patterns because the SEM technique determines the diameter from surface of the particle, while the XRD technique measures the single crystal grain of each particle; the major reasons for the difference in the particles sizes are the broad size distribution of the nanoparticles (Jensen *et al.*, 2006).

The elemental mappings are shown in Figs 1(c-e). EDX analysis of bio-ZnO sample is attached with their respective FESEM spectra (Fig. 1f) and it clearly shows the presence of Zn and O confirming the presence of ZnO with little impurity of carbon, which may have come from the leaf extract.

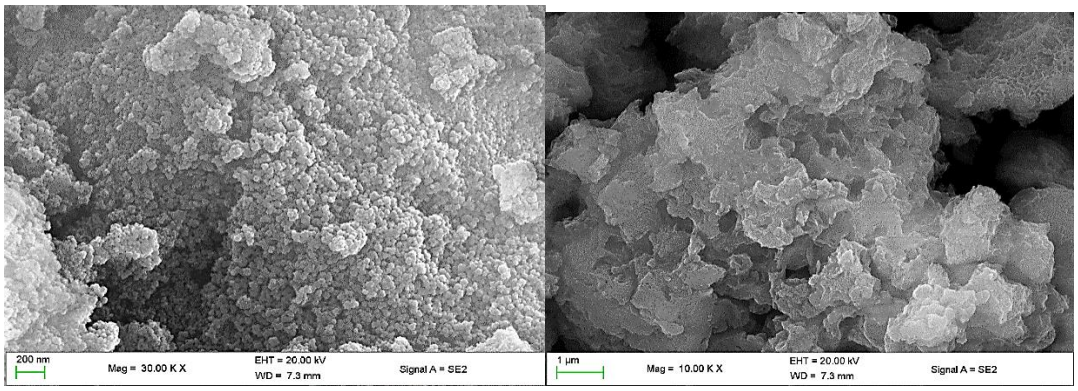

(a) **(b)**

Fig. 1(a-b). FESEM images of *S. indica* synthesized BioZnO nanoparticles at different magnifications

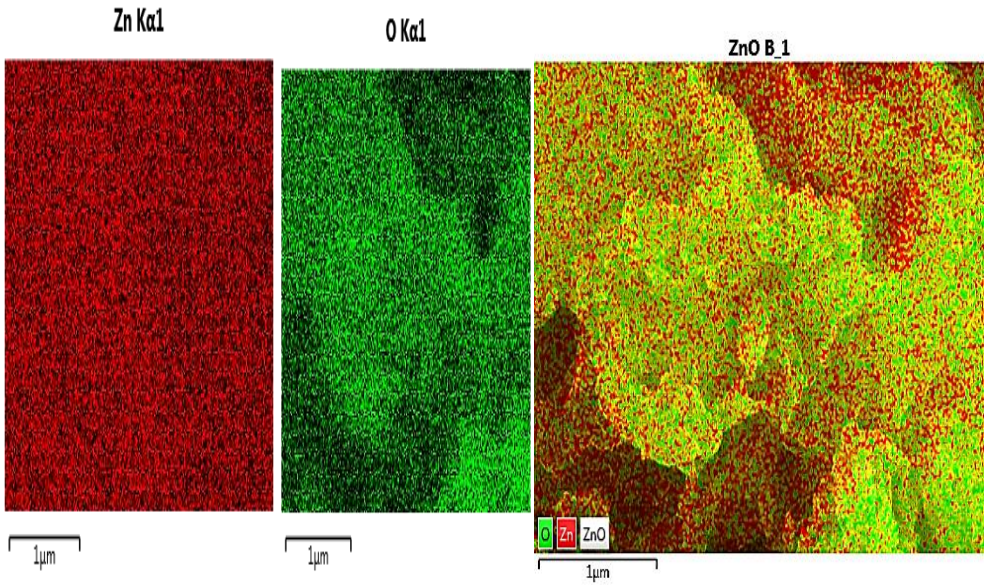

(c) (d) (e)

Fig. 1 (c-e). Elemental mappings of bioZnO

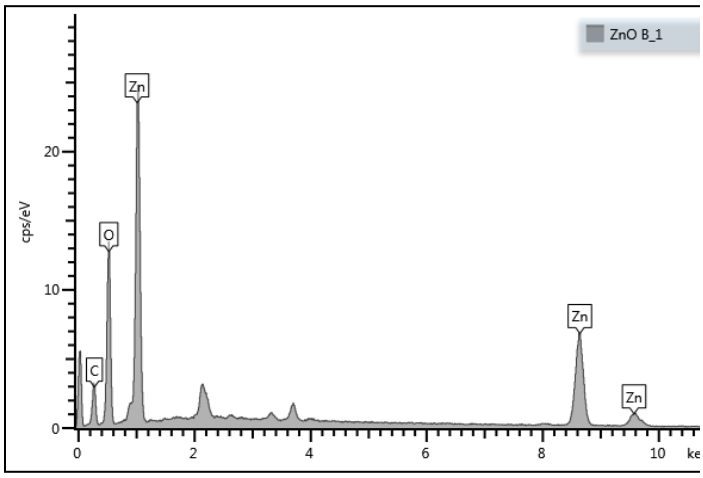

ZnO B_1	Wt%	Wt% Sigma
C	25.65	0.51
O	31.96	0.34
Zn	42.39	0.39
Total	100.00	

Fig. 1f. EDX spectra of Synthesized BioZnO nanoparticles

3.1.2 FESEM with EDX images of Biomagnetite nanoparticles

The FESEM images of the biomagnetite nanoparticles are shown in Fig. 2 (a-b). The images revealed a sheet-like layer that appeared clumped and cracked, which might be due to the thickening properties of the snake weed (*S. indica*) or the presence of hydroxyl groups from the extract (Venkateswarlu and Yoon, 2015). Besides, the tendency of agglomeration is not surprising as the synthesized biomagnetite-NPs were quite tiny in size. The average grain size according to SEM image was (1-4) nm which is in agreement with the result obtained from the XRD. The image obtained through EDX analysis and elemental mappings as shown in Fig. 2(c-f)

confirmed the appearance of Fe_3O_4 nanoparticles by indicating Fe-O group, and carbon, which may have originated from the leaf extract.

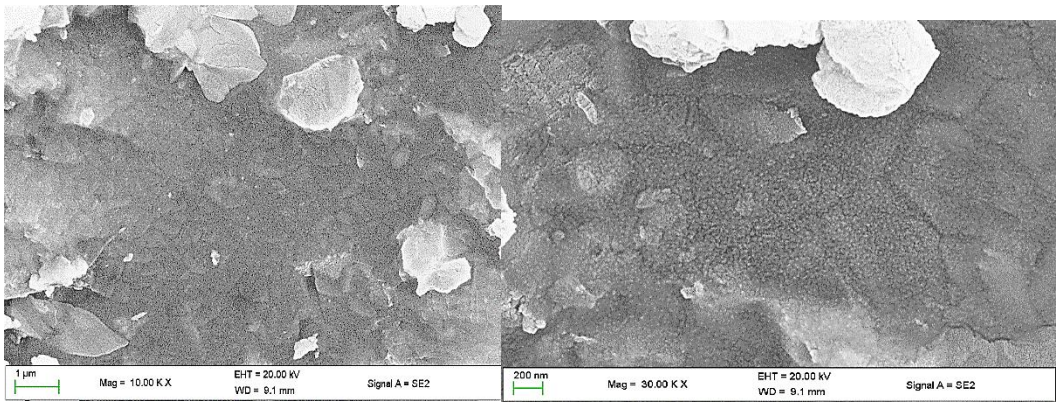

(a) **(b)**

Fig. 2(a - b). FESEM images of synthesized nano biomagnetite at different magnifications

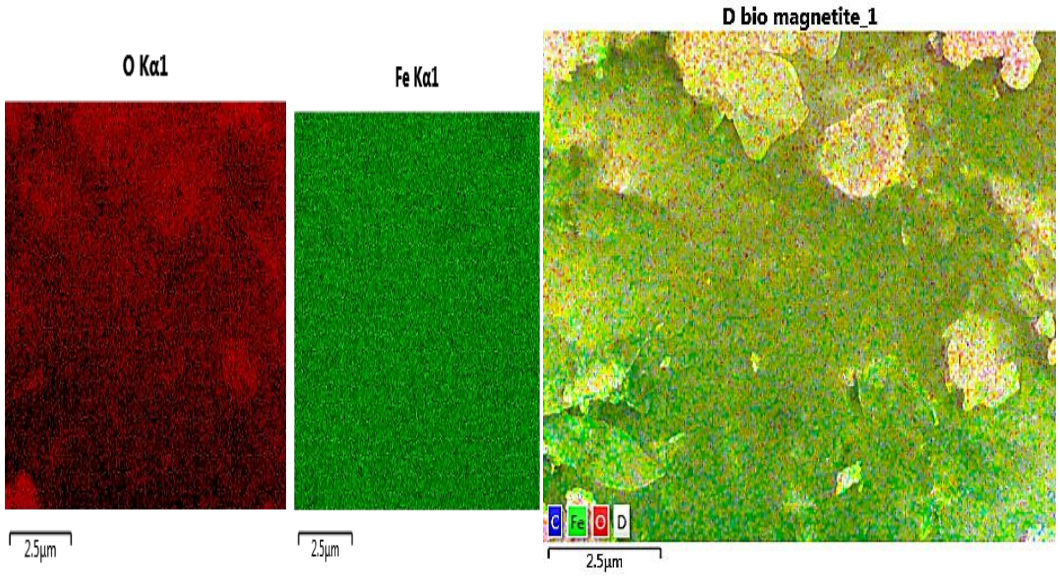

(c) **(d)** **(e)**

Fig. 2 (c-e). Elemental mapping of Biomagnetite

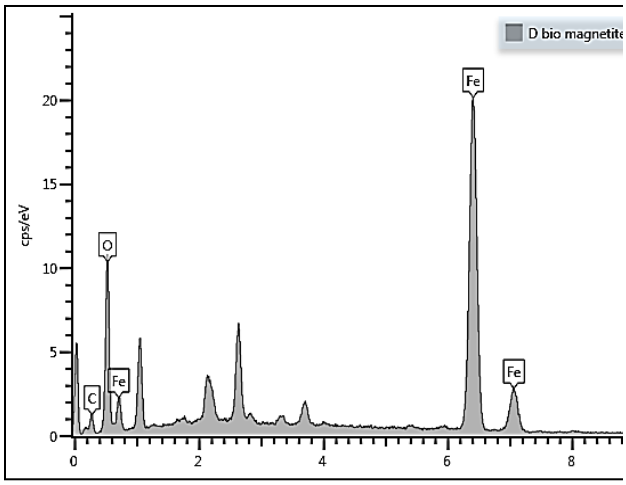

D bio magnetite_1	Wt%	Wt% Sigma
C	10.22	0.59
O	21.56	0.30
Fe	68.22	0.51
Total	100.00	

Fig. 2f EDX spectra of synthesized bio-Magnetite nanoparticles

3.2 XRD ANALYSIS

3.2.1 XRD Patterns of Bio-ZnO

In the bio-ZnO XRD patterns (Fig. 3), the presence of ZnO peaks along with other peaks were observed in the spectrum which indicates that the ZnO nanoparticles formed were completely capped by the biomolecules of the leaf extract. The sharp and narrow diffraction peaks indicate that the product is well crystalline in nature. The calculated average crystallite size of the powder particles was 3 nm.

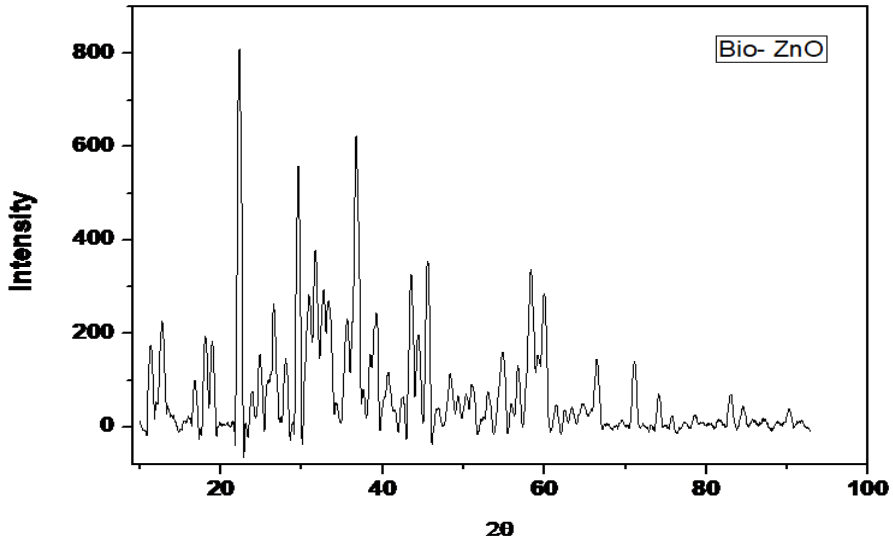

Fig. 3. XRD pattern of synthesized *S. indica* bioZnO nanoparticles

3.2.2 XRD Patterns of Bio-Magnetite

The XRD patterns of biomagnetite (Fig. 4) showed multiple peaks different from those of magnetite. This implies that the magnetite nanoparticles were mainly amorphous and capped by biomolecules extracted from *Starchytarpheta indica*. Hence the capping biomolecules might be the reason for not detecting the formed iron oxides (Luo *et al.*, 2014). Another reason could also be the incomplete magnetic separation during biosynthesis. However, the very sharp and broad diffraction peaks indicate that the product is well crystalline in nature. Calculations were performed according to the Scherrer equation and calculated results showed that the average crystallite size of the synthesized biomagnetite was 0.026 nm.

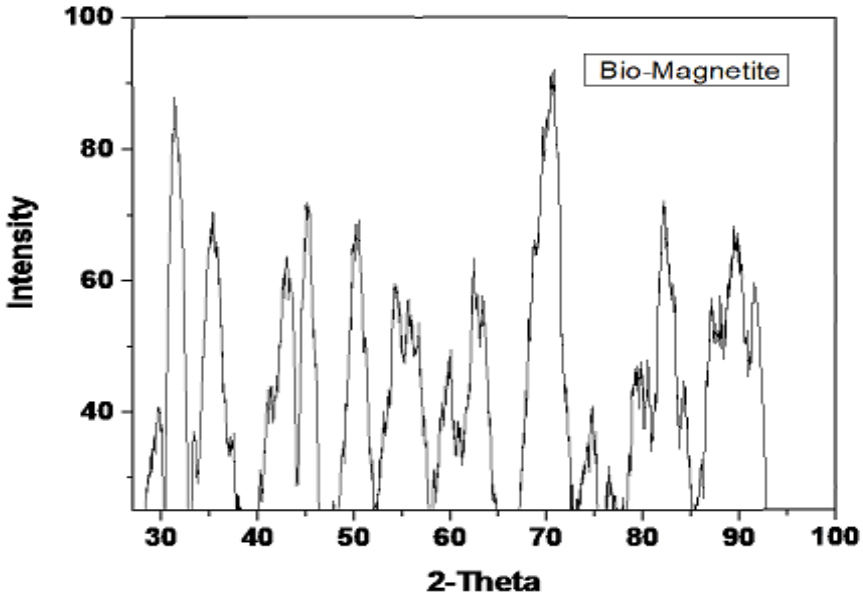

Fig. 4. XRD pattern of synthesized *S. indica* biomagnetite nanoparticles

Technium Vol. 2, Issue 5 pp.49-61 (2020)
ISSN: 2668-778X
www.techniumscience.com

3.3 FTIR Analysis

3.3.1 FTIR spectra of *S. Indica* extract

The FT-IR spectra of *S. indica* leaf extract is shown in Fig. 5. The absorption bands at wavelengths of 3761 and 3385 cm^{-1} correspond to O-H stretching vibrations of polyols. Peaks at 2919 and 2850 cm^{-1} also represent C−H aliphatic stretching of polyols. The sharp peak located at 1639 cm^{-1} represents C=C stretching vibrations of aromatic rings. Stretching vibrations present at 1413 and 1381 cm^{-1} are associated with O−H and C−OH vibrations of polyols, respectively. Stretching vibrations located at 663 cm^{-1} is attributed to N−H stretching vibrations of amines. The small peaks observed at 1730 and 1381 cm^{-1} may be attributed to C=O stretching vibrations of carboxylic acid. These bands indicate the abundance of polyols (phenolic acid and flavonoids), terpenoids and protein compounds in *S. indica* leaf extract, and may have largely contributed to the reduction of zinc salt to its nanoparticles.

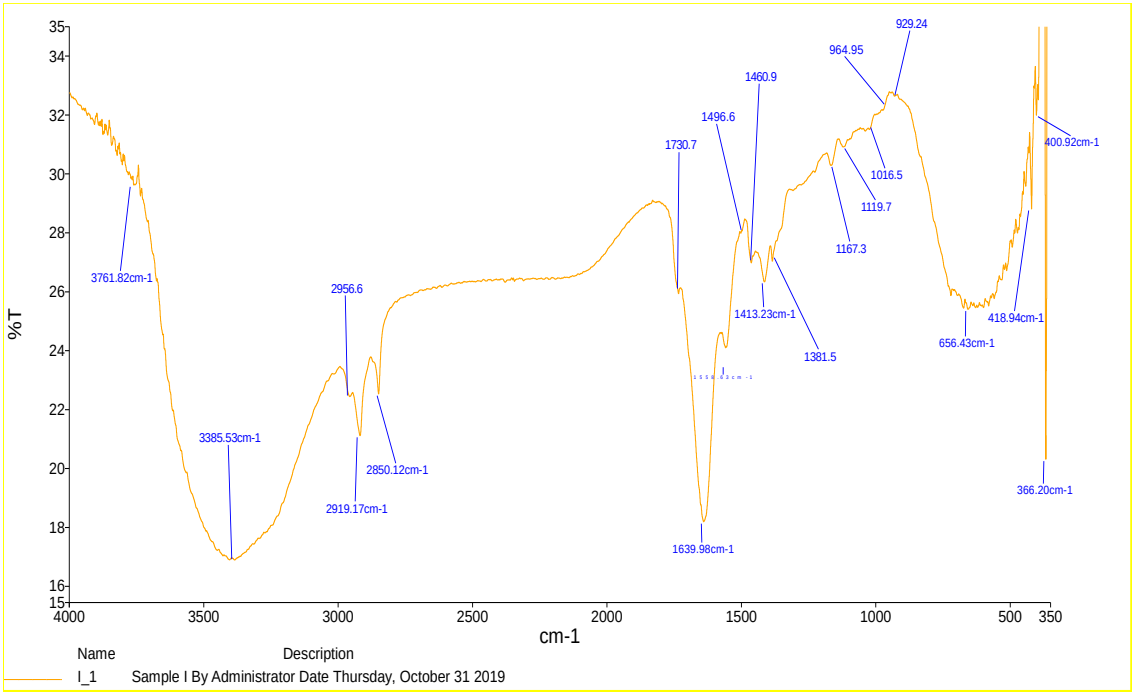

Fig. 5. FTIR spectrum of the chloroform extract of *S. Indica*

3.3.2 FTIR spectra of synthesized bio-ZnO nanoparticles

FTIR spectra of biosynthesized ZnO NPs (Fig. 6) shows shifts in absorption bands at 3975 cm^{-1}, 3392 cm^{-1}, 2936 and 2171 cm^{-1}, 1634 and 1551 cm^{-1}, 1493 and 1403 cm^{-1}, 836 cm^{-1} and 472 cm^{-1} respectively. The peaks in the region between 600 and 400 cm^{-1} correspond to M–O (Zn-O), while the band at 472 cm^{-1} confirms stretching vibrations of zinc oxide NPs.

Technium Vol. 2, Issue 5 pp.49-61 (2020)
ISSN: 2668-778X
www.techniumscience.com

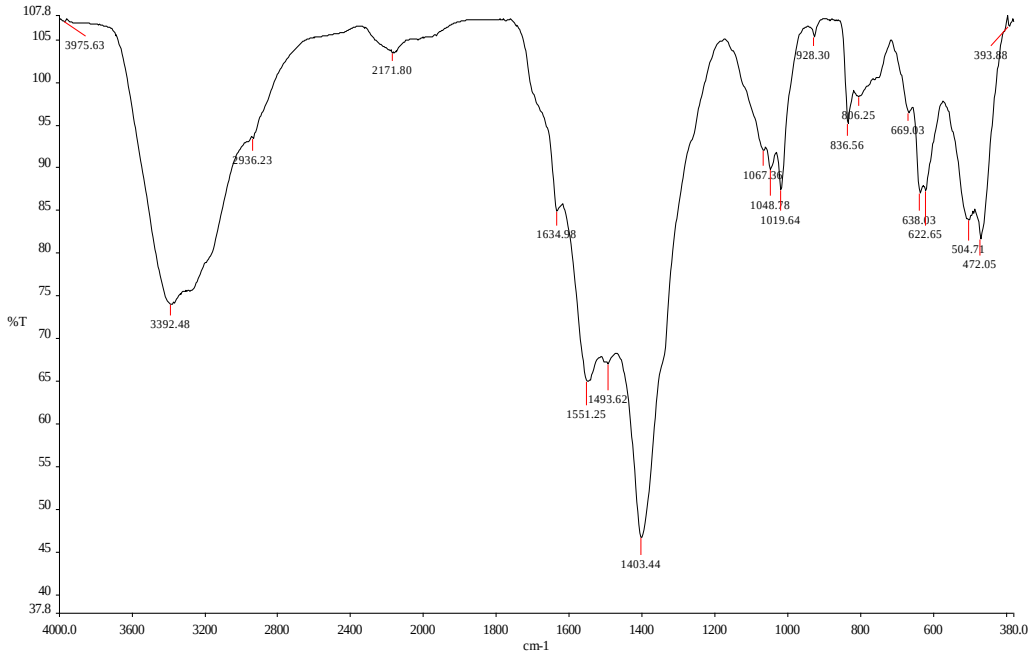

Fig. 6. FTIR spectrum of S. *Indica* synthesized ZnO nanoparticles before adsorption

3.3.3 FTIR spectra of synthesized bio-magnetite nanoparticles

The FT-IR spectrum of *S. indica* leaves extract (Fig. 5), indicated the presence of polyphenols and other biomolecules in the *S. indica* leaves extract and these biomolecules may have participated in the formation of magnetite nanoparticles. Fig. 7 indicates the appearance of the new peak at 589 cm^{-1} which is the typical characteristic absorption peak of magnetite nanoparticles.

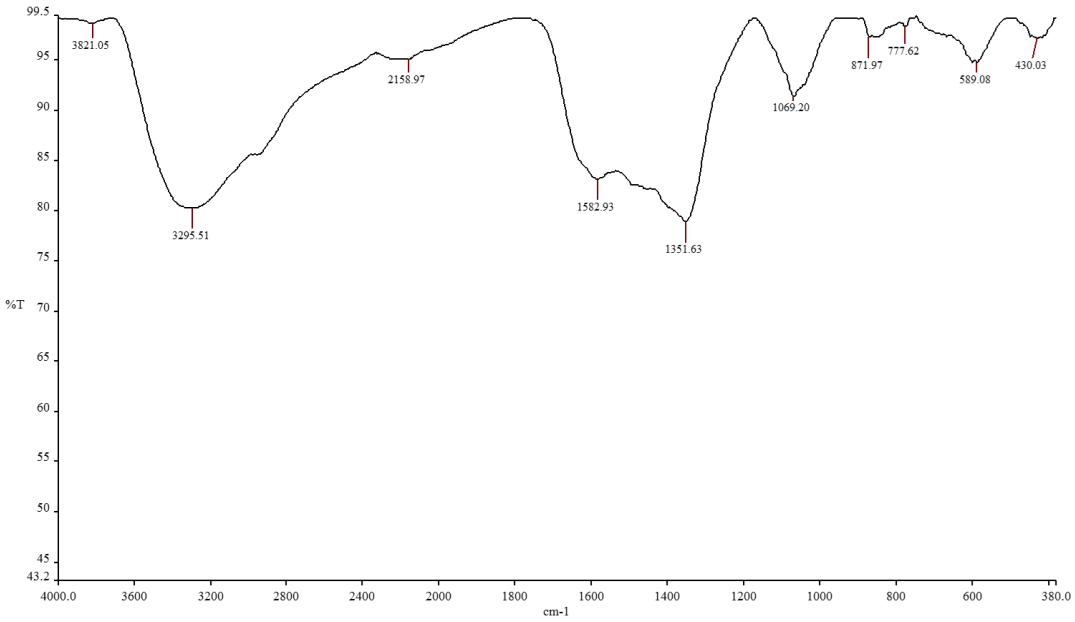

Fig. 7. FTIR spectrum of S. *indica* synthesized Bio-magnetite nanoparticles

The broad bands at 3821 and 3295 cm^{-1} are assigned to O-H (polyphenolic group) stretching, the weak band at 2158 cm^{-1} corresponds to C–H stretching and a band at around 1582 cm^{-1} can be attributed to the C=C ring stretching in polyphenols. The band at 1351 cm^{-1} corresponds to the C-N stretching vibrations while the medium peak at 1065 cm^{-1} may be attributed to the stretching vibration of C–O–C. Several other peaks in the spectral range 800–1800 cm^{-1} may also be attributed to the polyphenols that were likely present at the surface of iron nanoparticles.

4. Conclusion

The potential of snake weed extract as a reducing and capping agent in the biosynthesis of metal oxide nanoparticles has been investigated. Snake weed extract is an efficient and effective reducing and capping agent for the formation of ZnO and magnetite nanoparticles. This is an economical and environmentally friendly process. ZnO and magnetite nanocomplexes obtained appeared spherical and sheet-like respectively, with some degree of agglomeration. The crystallite sizes were 3 and 0.026 nm for both ZnO and Iron nanocomplexes. EDX analysis showed high percentages Zn and Iron elemental components that is consistent with the FESEM result obtained. Finally, the snake weed extract has been shown to contain a rich variety of polyphenols as indicated by the FTIR spectra, which is believed to have greatly enhanced the metal oxide nanocomplex formation. Further research in the reaction mechanism of reduction and stabilization process by the plant extracts is recommended.

References

Abou El-Nour K. M. M., Eftaiha, A., Al-Warthan, A and Ammar, R. A. A (2010) Synthesis and applications of silver nanoparticles. *Arab J Chem* 3:135–140

Ahmmad, B. Leonard, K and Islam, M. S. (2013). "Green synthesis of mesoporous hematite (α-Fe_2O_3) nanoparticles and their photocatalytic activity," *Advanced Powder Technology*, 24(1), 160–167.

Ali, K., Dwivedi, S., Azam, A., Saquib, Q., Al-Said, M., Alkhedhairy, A., and Musarrat, J. (2016). Aloe vera extracts functionalized zinc oxide nanoparticles as nanoantibiotics against multi-drug resistant clinical bacterial isolates. *Journal of Colloid and Interface Science*. 472: 145-156.

Al-Ruqeishi, M. S., Mohiuddin, T and Al-Saadi, L. K (2016). Green synthesis of iron oxide nanorods from deciduous Omani mango tree leaves for heavy oil viscosity treatment. *Arab J. Chem*. https://doi.org/10.1016/j.arabjc.2016.04.003

Asanithi, P., Chaiyakun, S. and Limsuwan, P (2012) Growth of silver nanoparticles by DC magnetron sputtering. *J Nanomate*r. 2012:963609

Barreto, J. C., Trevisan, M. T., Hull, W. E., Erben, G., Brito, E. S. D., Pfundstein, B., Würtele, G, Spiegelhalder, B., and Owen R. W. (2008). Characterization and quantitation of polyphenolic compounds in bark, kernel, leaves, and peel of mango (*Mangifera indica* L). *J Agric Food Chem* 56: 5599–5610.

Felicien, M. (2016). "Comparative hypoglycemic activity of flavonoids and tannins fractions of *Stachytarpheta indica* (L.) Vahl leaves extracts in guinea-pigs and rabbits." *Int. J. Pharm. Pharmaceutical Res.* 5: 48-57.

Ghorbani, P., Soltani, M., Homayouni-Tabrizi, M., Namvar, F., Azizi, S., Mohammad, R., Boroumand and Moghaddam, A. (2015). Sumac silver novel biodegradable nano composite for bio-medical application: Antibacterial activity. *Molecules*. 20:12946–12958.

Garadkar, P. K. M., Gawade, V., Gavade, N., Shinde, H., Babar, S. B and Kadam, A. (2017). Green synthesis of ZnO nanoparticles by using Calotropis procera leaves for the photodegradation of methyl orange. *Journal of Materials Science: Materials in Electronics.* 1-7.

Gnanasangeetha, D. and Thambavani, S (2013a). ZnO nanoparticle entrenched on activated silica as a proficient adsorbent for removal of As^{3+} *Int J Res Pharma Biomed Sci.* 4(4):1295–1304

Gnanasangeetha, D. and Thambavani, S (2013b). ZnO nanoparticle entrenched on activated silica as a proficient adsorbent for removal of As^{3+} *Int J Res Pharma Biomed Sci.* 4(4):1295–1304

Jensen, H., Pedersen, J. H., Jorgensen, J. E., Skov Pedersen, J., Joensen, K. D., Iversen, S. B and Sogaard, E. G. (2006). Determination of size distributions in nanosized powders by TEM, XRD, and SAXS, *Journal of Experimental Nanoscience*, 1(3): 355 - 373.

Luo, F., Chen, Z., Megharaj, M. and Naidu, R. (2014). Biomolecules in grape leaf extract involved in one-step synthesis of iron-based nanoparticles, *RSC Adv*., 4: 53467-53474.

Mahdavi, M., Ahmad, M., Haron, M. J, Namvar, F., Nadi, B., Rahman, M. and Amin, J. (2013). Synthesis, Surface Modification and Characterisation of Biocompatible Magnetic Iron Oxide Nanoparticles for Biomedical Applications. *Molecules (Basel, Switzerland).* 18: 7533-7548.

Manna, J, Begum, G. Pranay K., Kumar, S., Misra, R. and Rana, K (2013). Enabling Antibacterial Coating via Bioinspired Mineralization of Nanostructured ZnO on Fabrics under Mild Conditions, *ACS Appl. Mater. Interfaces* 5, 4457−4463.

Mihir, H., Siddhivinayak, B. and Rakesh, K. (2014). Plant-Mediated Green Synthesis of Iron Nanoparticles *Journal of Nanoparticles*, 14, 9 http://dx.doi.org/10.1155/2014/140614

Nayantara, P. K. (2018). Biosynthesis of nanoparticles using eco-friendly factories and their role in plant pathogenicity: a review, *Biotechnology Research and Innovation*, 2(1): 63-73.

Oudhia, A., Kulkarni, P., and Sharma, S. (2015). Green synthesis of ZnO nanotubes for bioapplications. *Int J Curr Eng Technol* 1, 280–281.

Ramesh, M., Anbuvannan, M. and Viruthagiri, G (2015). Green synthesis of ZnO nanoparticles using *Solanum nigrum* leaf extract and their antibacterial activity. *Spectrochim Acta A Mol Biomol Spectrosc* 13, 864–870.

Roldán, M. V., Pellegri, N and de Sanctis, O (2013). Electrochemical method for Ag-PEG nanoparticles synthesis. *J Nanopart* 2013:524150

Sahoo, S.R., Dash, R. and Bhatnagar, S. (2014). Phytochemical screening and bioevaluation of medicinal plant *Stachytarpheta indica (*L.) Vahl. *Pharmacology & Toxicology Research*. 1. 1-5.

Sangeetha, G., Rajeshwari, S. and Venckatesh, R (2011). Green synthesis of zinc oxide nanoparticles by *Aloe barbadensis miller* leaf extract: structure and optical properties. *Mater Res Bull* 46 (12): 2560–2566.

Shah, M., Fawcett, D., Sharma, S., Tripathy, S. K. and Poinern, G. (2015). Green Synthesis of Metallic Nanoparticles via Biological Entities. *Materials (Basel, Switzerland)*, *8*(11): 7278–7308.

Siddiqi, K. S., Husen, A. and Rao, R. A. K (2018). A review on biosynthesis of silver nanoparticles and their biocidal properties. *J Nanobiotechnol* 16:14

Thakkar, K. N. Mhatre, S. S. and Parikh, R.Y (2010). Biological synthesis of metallic nanoparticles, *Nanomedicine*, 6(2), 257–262

Venkateswarlu, S, and Yoon, M. (2015). Surfactant-free green synthesis of Fe_3O_4 nanoparticles capped with 3, 4-dihydroxyphenethylcarbamodithioate: stable recyclable magnetic nanoparticles for the rapid and efficient removal of Hg(II) ions from water. *J. Chem. Soc. Dalton Trans* 44(42):18427–18437.